signals

MDPI

Article

The Use of Instantaneous Overcurrent Relay in Determining the Threshold Current and Voltage for Optimal Fault Protection and Control in Transmission Line

Vincent Nsed Ogar *, Sajjad Hussain and Kelum A. A. Gamage

Department of Electrical and Electronic Engineering, James Watt School of Engineering, University of Glasgow, Glasgow G12 8QQ, UK

* Correspondence: v.ogar.1@research.gla.ac.uk

Abstract: When a fault occurs on the transmission line, the relay should send the faulty signal to the circuit breaker to trip or isolate the line. Timely detection is integral to fault protection and the management of transmission lines in power systems. This paper focuses on using the threshold current and voltage to reduce the time of delay and trip time of the instantaneous overcurrent relay protection for a 330 kV transmission line. The wavelet transforms toolbox from MATLAB and a Simulink model were used to design the model to detect the threshold value and the coordination time for the backup relay to trip if the primary relay did not operate or clear the fault on time. The difference between the proposed model and the model without the threshold value was analysed. The simulated result shows that the trip time of the two relays demonstrates a fast and precise trip time of 60% to 99.87% compared to other techniques used without the threshold values. The proposed model can eliminate the trial-and-error in programming the instantaneous overcurrent relay setting for optimal performance.

Keywords: circuit breaker; overcurrent relay; faults; threshold current; threshold voltage; transmission line

Citation: Ogar, V.N.; Hussain, S.; Gamage, A.A.G. The Use of Instantaneous Overcurrent Relay in Determining the Threshold Current and Voltage for Optimal Fault Protection and Control in Transmission Line. *Signals* **2023**, *4*, 137–149. https://doi.org/10.3390/signals4010007

Academic Editor: Francesco De Paulis

Received: 15 November 2022
Revised: 17 January 2023
Accepted: 3 February 2023
Published: 7 February 2023

1. Introduction

The power system's major and minor components are critical in transmitting electric supply from the generation site to the customer. However, the fault protective relay is the most crucial and sensitive of all these components. These comprise the overcurrent and overvoltage relay protection. Transmission line faults disrupt the consumer's power supply, which is inconvenient and could result in financial losses. Damage to the power system or a power outage at the consumer's end could result in financial losses. When a failure occurs on the transmission lines, it is critical to protect them [1]. Overcurrent protection is capable of operating under any fault condition. The relay's current pickup value must be higher than the maximum value of projected output or regular load flow situations. The overcurrent relay is commonly utilised in radial transmission and distribution systems [2]. In the event of an abnormal condition or fault, such as a short circuit, the protective relay de-energises the defective component of the distribution power system, preventing the rest of the system from being impacted [3]. The relays are established in cooperation to prevent the incidents mentioned earlier and their impact on customers. Because improper coordination can have significant implications for the electrical network, such as power outages, equipment damage, and utility station faults, properly coordinated relays are critical for the power system network. The current magnitude increases when the power system malfunctions, causing network damage [4]. The fault current is measured by the overcurrent relays and compared to predetermined threshold values. When the current level exceeds the threshold, a trip order is delivered, and the appropriate circuit breaker opens its contacts and isolates the faulted area after a predetermined time delay.

Some literature has recently proposed tools to aid transmission and distribution system protection based on overcurrent relay settings. In [5], an approach for fault calculation in imbalanced distribution systems was disclosed where the primary protective devices and functions employed in distribution systems have mathematical models. This method makes complete three-phase representations possible, and the solution is achieved directly in phase coordinates. In [6], an integrated optimising model for current relay coordination with tough, practical limitations based on a gradient-based optimiser was analysed, and the model was used to enhance the protection coordination of the transmission and distribution network with some constraints such as false tripping actions. In [7,8], this study describes a computational tool that was created to automatically calculate the adjustments of all distribution network protection devices to acquire the best technological application, optimise its performance, and make protection studies easier. Ref. [9] presents a straightforward method in which two-phase faults were diagnosed based on the negative sequence current value, and the operating conditions of the suggested criteria arising from negative and zero sequence currents were automatically selected based on the three-phase short-circuit criterion. However, the paper fails to introduce the controller operation of the circuit breaker for adequate tripping of the transmission line. In another paper [10], based on a real-time estimation of the Thevenin equivalent circuit (TEC), the methodology determines the protection setting settings. The estimation process used the voltage and current values in the positive sequence and a system of nonlinear equations that were solved repeatedly using the Gauss–Newton method. Additionally, in [11], the implementation of a new adaptive protection method to set online overcurrent relays in distribution networks was implemented for miscoordination of the overcurrent relay.

The connecting and disconnecting of transmission lines and their components are critical to changing fault currents' magnitude and flow direction. Change in the network configuration also leads to a disturbance in the overcurrent relay functionality. The fault current signal affects the power transformer and other components when a fault occurs in the transmission line. Therefore, the circuit breaker needs to open immediately to prevent damage to the installation. The fault current magnitude is greater than the standard load current, so the relay should be signed to operate and trip the circuit breaker for all currents above the relay settings. The overcurrent relay needs a backup relay for proper coordination such that, if one fails to trip, the backup relay will trip automatically.

To protect the transmission lines against multi-phase faults, the overcurrent protection criterion with a fixed current threshold and time-independent operation on fault current value is frequently utilised. Usually, two of these protection relays are currently deployed. The situation right now acting as the time-delay short-circuit, and the initial line of defence overload prevention identified by the $I >$ symbol, must adhere to the subsequent conditions,

$$I_{min} > I_{pr} > I_{st}, \tag{1}$$

where I_{min} is the minimum short-circuit phase current of the transmission line with $I >$ protection, I_{pr} is the threshold value of the current protection, and I_{st} is the steady state component of the highest load current of the line [9]. Such protection relays respond only to phase current values and are typically definite minimum time (DMT) overcurrent relays configured to meet selectivity requirements.

According to the literature reviewed above, this paper proposed the following approaches:

1. The use of wavelet transforms to determine the threshold voltage and current of faulty transmission lines;
2. A designed model to determine the tripping time and the operating time of instantaneous over current relay at different fault-resistant values;
3. A protection scheme was designed to evaluate and determine the response time of relays in different zones.

Contribution of the Proposed Algorithm

The proposed algorithm performs better than those mentioned in the literature due to its speed in obtaining the threshold values for setting the overcurrent and overvoltage relay. Additionally, fault signals are accompanied by noise. Therefore, using the wavelet transform to determine the threshold current and voltage helps denoise the signal to attain stability in the system. It also serves as a fast gateway for instantaneous relay settings for optimal protection of transmission and distribution line fault detection and isolation with the use of a circuit breaker.

2. Proposed Algorithm

The proposed model uses the discrete wavelet transform to generate the threshold current and voltage for the overcurrent relay setting. This method is a fast and reliable process to determine the pickup current, minimum and maximum threshold current and voltage for the fast and accurate detection of transient or overcurrent faults in the transmission line. The proposed model improves the relay protection level, reduces the operating time of the relay and better coordinates between the primary and backup relay.

2.1. Wavelet Transform

The wavelet transform (WT) is a mathematical tool with which to analyse the power system transient signals. It extends a single prototype function to break up a signal into different scales with different levels of resolution. It shows how the signal looks locally in both the time and frequency domains. This wavelet transform capability is used to locate, classify, and detect fault conditions. The basic idea behind wavelet analysis is to choose an appropriate wavelet function known as the "mother wavelet" and then analyse it using shifted and dilated versions of this wavelet [12]. The fault signals are transformed into different frequency bands using the discrete wavelet transform and the Daubechies wavelet transform in this method, which can then be used to identify the faults. These signals can be represented in terms of both the scaling and wavelet function, as shown in the equation below;

$$f(t) = \Sigma_n C J^n \Phi^{t-n} + \Sigma_n \Sigma_{j=0}^{J} d_j(n) 2^{\frac{j}{2}} \Psi(2^j t - n), \tag{2}$$

where c_j represents the J level scaling coefficient and d_j represents the j level wavelet function. $\Phi(t)$ is the scaling function, $\Psi(t)$ is the wavelet function, J is the highest wavelet level, and t is the time. Each wavelet is created by the scaling and translation operations of the mother wavelet [12]. The continuous WT for a given signal $x(t)$ to the parent wavelet $\Psi(t)$ is shown in Equation (2):

$$CWT_\Psi x(a,b) = W_x(a,b) = \int_{-\infty}^{\infty} x(t) \Psi a, b^{(t)} dt, \tag{3}$$

where $\Psi a, b(t) = \mid a \mid^{\frac{1}{2}} \Psi(\frac{t-b}{a})$, a (scale) and b (translation) are real numbers. For discrete-time systems, the discretion process leads to the time-discrete wavelet series given as

$$DWT_\Psi x(m,n) = \int_{-\infty}^{\infty} x(t) \Psi m, n^{(t)} dt, \tag{4}$$

where $\Psi m, n(t) = {a_0}^{\frac{-m}{2}} \Psi\left(\frac{t - n b_o a_0^m}{a}\right)$, $a = {a_0}^m$ and $b = n b_0 {a_0}^m$.

2.2. Data Acquisition

A 330 kV, 50 Hz, 500 km transmission line was modelled using MATLAB/SIMULINK, and 11 different types of faults were induced in the model, and the fault current data were collected and recorded, as shown in the table below. A wavelet transform syntax was applied to obtain the maximum coefficient current for phases A,B and C. $[C, 1]$ = wavedec(x,n, wname), where wavedec is the function which decomposes the signal. X is the signal

generated, n is the wavelet layer, wname is the name of wavelet type and C is the output wavelet decomposition vector, while l is the number of coefficients by layer.

The voltage and current of the grid experience transients when faults occur. Using a discrete wavelet transform to analyse these transients, the defect can be categorised [13]. The zero sequence and phase transient currents are analysed to determine the fault that occurred. Wavelet transform identifies the phase-related fault by calculating the energy of transients linked to each phase and ground.

MATLAB/Simulink was used to simulate the model using the RLC load at the receiving end, while the three-phase source block was used at the sending end; 330 kV, 500 km, 50 Hz and a three-phase transmission line were used for the model. The coefficient of each fault type was calculated and compared with the threshold value by checking the maximum and minimum threshold values.

Table 1 shows the maximum coefficient value of the different fault types. In contrast, Table 2 represents the maximum and minimum threshold values for each current fault phase.

Table 1. Faulty current and voltage data in kA and kV.

Fault Types	Coeff of I_a	Coeff of I_b	Coeff of I_c	Coeff of V_a	Coeff of V_b	Coeff of V_c
ABC-G	533.0974	495.1115	575.3335	0.0000	0.0000	0.0000
ABC	395.1943	587.4911	474.7873	−0.0001	0.0000	0.0001
(AB-G)	338.5069	531.6202	32.9732	0.6655	−1.6882	1.0227
(AC-G)	306.5768	22.3418	620.4303	1.5501	−0.1691	−1.3810
(BC-G)	26.1066	608.8079	294.0561	−1.2685	1.6153	−0.3468
(A-B)	855.3816	385.9281	17.8156	−1.2792	1.6102	−0.3311
(A-C)	299.0803	19.8595	574.5684	−1.2897	1.6050	−0.3154
(B-C)	15.3783	420.5652	355.8047	−1.3001	1.5996	−0.2996
(A-G)	307.6007	39.5083	20.8305	−1.3103	1.5941	−0.2838
(B-G)	32.6032	199.6292	28.3545	−1.3205	1.5885	−0.2680
(C-G)	15.1679	28.6647	364.3873	0.4383	−1.6423	1.2040
No Fault	10.6870	15.1958	23.0105	1.4530	0.0390	−1.4920

Table 2. Threshold value of current at different fault locations.

Fault Types	Threshold of I_a (kA)		Threshold of I_b (kA)		Threshold of I_c (kA)		Threshold of Ground Current (kA)
	Max	Min	Max	Min	Max	Min	
ABC-G							18.6876
ABC							56.9488
AB-G					531.6202	32.9732	25.7012
AC-G			620.4303	22.3418			15.5710
BC-G	608.8079	26.1066					20.9355
A-B					855.3816	17.8156	28.2445
A-C			574.5684	19.8595			34.5217
B-C	420.5652	15.3783					16.8326

Table 2. *Cont.*

Fault Types	Threshold of I_a (kA)		Threshold of I_b (kA)		Threshold of I_c (kA)		Threshold of Ground Current (kA)
	Max	Min	Max	Min	Max	Min	
A-G			307.6007	39.5083	307.6007	20.8305	18.3399
B-G	199.6292	32.6032			199.6292	28.3545	24.7174
C-G	364.3873	15.1679	364.3873	28.6647			15.5710
No-Fault	23.0105	10.6870	23.0105	15.1958	23.0105	23.0105	13.0455

3. Modelling of the High Sensitive Overcurrent Relay

This protection switchgear block contains a current transformer, a circuit breaker (52) and an IDMT overcurrent relay (51P) that operate when the current exceeds the relay's predetermined value. This relay operates based on the IEC 60255 standard for normal inverse IDMT trip characteristics, as seen in Figure 1. It also contains a phasor measurement unit (PMU) and two supply and switching units (SSU) connected to a separate bus with 10 kA, 6 kA and 4 kA faults. These fault values are obtained from Tables 1 and 2. The input voltage was a 330 kV high voltage transmission line, and an output display of the relay status showed the tripping time and fault current.

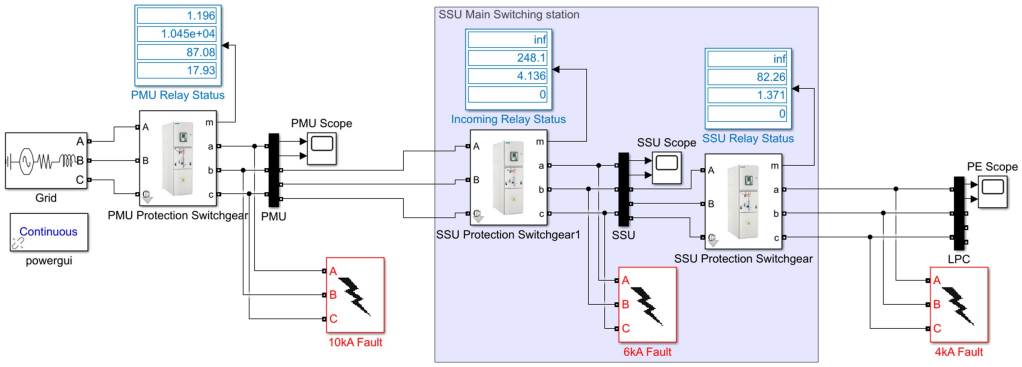

Figure 1. Instantaneous overcurrent relay block model.

The overcurrent relay activates when the fault current exceeds the relay pickup current. The pickup current is calculated in operating time, and the inverse definite minimum time (IDMT) is defined as the amount of time taken before the circuit breaker trips when an overcurrent is initiated in a circuit or transmission line are also calculated. The operating time is defined as a fixed parameter such that an instantaneous overcurrent relay is produced when the operating time is set to zero [14]. This can be illustrated in Figure 2 below and, to calculate the trip time, the IEEE C37.112-1996 equation for the trip time used is given as:

$$t(I) = TD\left(\frac{A}{(\frac{1}{I_s})^p - 1} + B\right), \tag{5}$$

where A is the time factor for the overcurrent trip, I is the actual current, Is is the relay pickup setting, p is the exponent for inverse time, and B is the time coefficient for the overcurrent trip. While the IEC 60255 IDMT trip curve equation is given by

$$t(I) = TMS\left(\frac{k}{(\frac{1}{I_s})^\alpha - 1}\right), \tag{6}$$

where α and k are the curve constants and seen in Table 3 below.

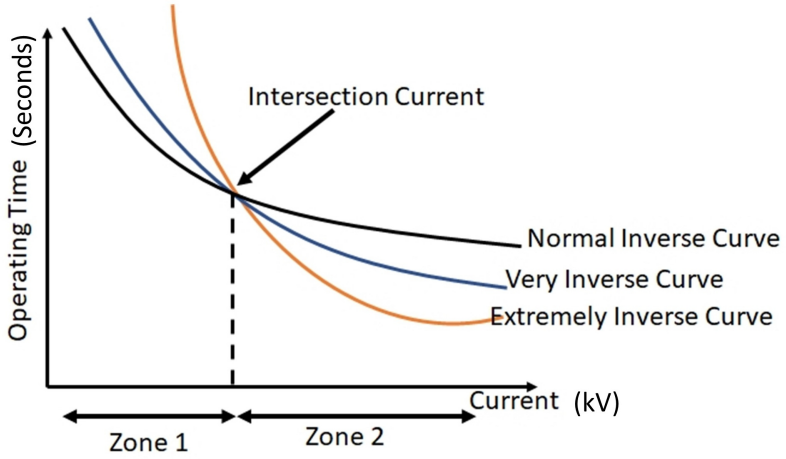

Figure 2. Instantaneous overcurrent relay block model.

Table 3. IDMT curve constant.

Curve Types	K	α
Normal Inverse Curve	0.140	0.020
Very Inverse Curve	13.5	1
Extremely Inverse Curve	80	2
Long-time Standard Curve	120	1

4. Results and Discussion

The threshold current or peak make current and the short circuit breaking current can be calculated by finding the RMS symmetrical current $i''k$; the peak make current for a single radial current is calculated using the peak factor k.

$$i_p = k\sqrt{2i''k}, \tag{7}$$

where $k = 1.02 + 0.98x10^{-3}\left(\frac{X}{R}\right)$.

$$Peakfactor = \sqrt{2}\left[1 + sin\left\{tan^{-1}(\frac{X}{R})\right\}exp\left\{\frac{-[\frac{\pi}{2} + tan^{-1}(\frac{X}{R})]}{\frac{X}{R}}\right\}\right], \tag{8}$$

where the $\frac{X}{R}$ is the system ratio at the fault point. The RMS current is given by I_rms total at $\frac{1}{2}$ cycle (KA),

$$I_rms = \sqrt{I + 2exp\left[-\frac{\frac{\pi}{2}}{\frac{X}{R}}\right]}XI_rms, \tag{9}$$

at $\frac{1}{2}$ cycle(KA) and $\frac{X}{R} = \left(\frac{X_c^p}{R_c^p}\right) \times \frac{f}{f_c}$ for single phase to Earth faults. f is the normal frequency and f_c is the equivalent frequency.

The model generated the threshold current when the fault resistance was set at 0.01 Ω, 50 Ω and 100 Ω. The response times of the three different relays were also analysed, as seen in Tables 4–6.

Table 4. Threshold current at fault resistance of 0.01 Ω.

Fault Types	**Fault Resistance = 0.01 Ω**		
Three-phase to ground fault	Relay 1	Relay 2	Relay 3
Threshold Current (kA)	259	8.524	2.826
TMS (Seconds)	2.991	0.1421	0.04709
Trip Time (Seconds)	0.01	0.01	0.01
Double phase to ground fault	Relay 1	Relay 2	Relay 3
Threshold Current (kA)	358.9	13.25	4.424
TMS (Seconds)	2.991	0.2208	0.07373
Trip Time (Seconds)	0.01	0.01	0.01
Single line to ground fault	Relay 1	Relay 2	Relay 3
Threshold Current (kA)	358.8	16.43	5.478
TMS (Seconds)	2.99	0.2739	0.0913
Trip Time (Seconds)	0.01	0.01	0.01

Table 5. Threshold current at fault resistance of 50 Ω.

Fault Types	**Fault Resistance = 50 Ω**		
Three-phase to ground fault	Relay 1	Relay 2	Relay 3
Threshold Current (kA)	358.7	355.8	117.9
TMS (Seconds)	2.989	5.93	1.966
Trip Time (Seconds)	0.01	0.9198	0.01
Double phase to ground fault	Relay 1	Relay 2	Relay 3
Threshold Current (kA)	358.7	355.7	118.3
TMS (Seconds)	2.989	5.929	1.971
Trip Time (Seconds)	0	0.9193	0
Single line to ground fault	Relay 1	Relay 2	Relay 3
Threshold Current (kA)	358.5	355.5	118.5
TMS (Seconds)	2.987	5.925	1.975
Trip Time (Seconds)	0	0.9185	0

The tripping time varied as the fault resistance changed from 0.01 Ω to 100 Ω at different fault conditions. In Table 4, when the fault resistance was at 0.01 Ω, the trip time was 0.01 s at the three relays and all the fault conditions. At the same time, it was quite different when the fault resistance changed to 50 Ω. The trip time was reduced to zero seconds at a double line to ground and a single line to ground fault at relays 1 and 3 with a variation in relay 2 of about 0.91 s as seen in Table 5. The time multiplier setting (TMS) for each of the relays was set at 1 s, 2 s and 5 s, and the error after tripping was about 0.9 s, which is minimal, as seen in Table 6 (0.98 s, 0.89 s and 0.96 s) for the three phases to ground fault. This can be seen in Figure3 A–C, where the TMS was set to 5 s, 2 s and 1 s, respectively.

A backup relay was added to the network for optimal system performance to prevent feedback faults. In instances where relay 1 failed to operate, it sent the signal to relays 2 and 3 for better coordination and protection.

Table 6. Threshold current at fault resistance of 100 Ω.

Fault Types	**Fault Resistance = 100 Ω**		
Three-phase to ground fault	Relay 1	Relay 2	Relay 3
Threshold Current (kA)	358.2	353.9	117.9
TMS (Seconds)	2.985	5.899	1.966
Trip Time (Seconds)	0	0.9149	0.9039
Double phase to ground fault	Relay 1	Relay 2	Relay 3
Threshold Current (kA)	358.1	353.8	118.3
TMS (Seconds)	2.984	5.897	1.971
Trip time (Seconds)	0	0.9145	0.9035
Single line to ground fault	Relay 1	Relay 2	Relay 3
Threshold Current (kA)	358	353.7	349.5
TMS (Seconds)	2.984	5.895	5.824
Trip Time (Seconds)	0	0.9136	0.9026

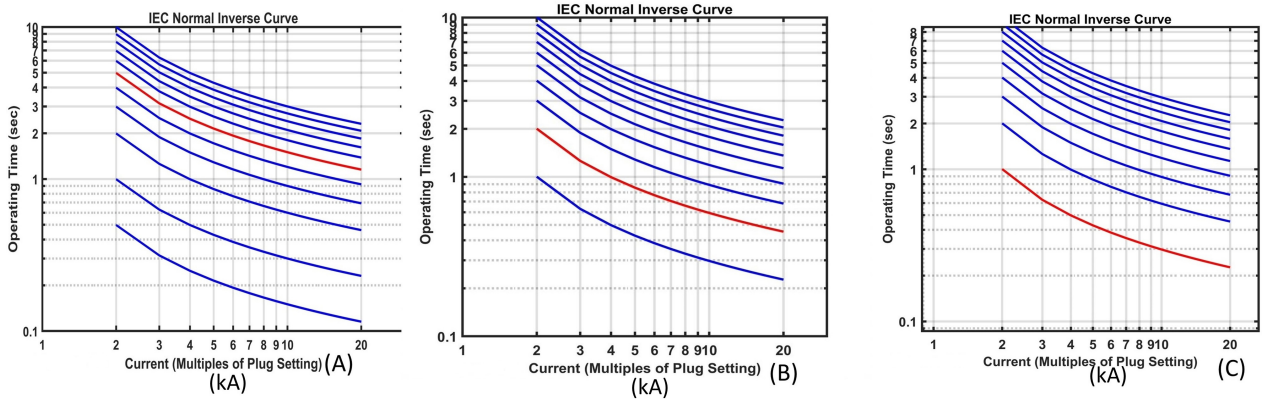

Figure 3. Time multiplier settings at 1 second.

The threshold current also varied as the fault resistance increased and was slightly different in the different fault types, as seen in Table 6, where the threshold current was an average of 358 kV in relay 1 and was slightly different in relay 3 of the single phase-to-ground fault.

Transmission line faults can be found and identified with less accuracy when there are noise signals. When choosing and extracting fault characteristics, noise signals such as voltage sag, transients, harmonics, and voltage interruption must be considered. In [15], the DWT was utilised for feature extraction, and the SVM was used for fault classification, with 100% accuracy when there was no disturbance and 98% and 95.6% accuracy when there was 30 dB and 20 dB noise, respectively. It is recommended that noise be removed using the DWT approach during fault extraction to obtain a denoised signal.

4.1. Validation of the Result Using the Threshold Current and Voltage with Other Models for the Sensitivity of TMS

Two scenarios were created in Figures 4 and 5 to show when three phase-to-ground faults were initiated to bus A and B, and the relay was applied in bus B while bus A was without a relay. In the implementation of the proposed model in Figure 4, at the maximum threshold current, the circuit breaker tripped at 0.05 s and was restored. When the relay was initiated, the line tripped at 0.04 s, and the operating time delay was 0.035 s, as seen in Figure 5.

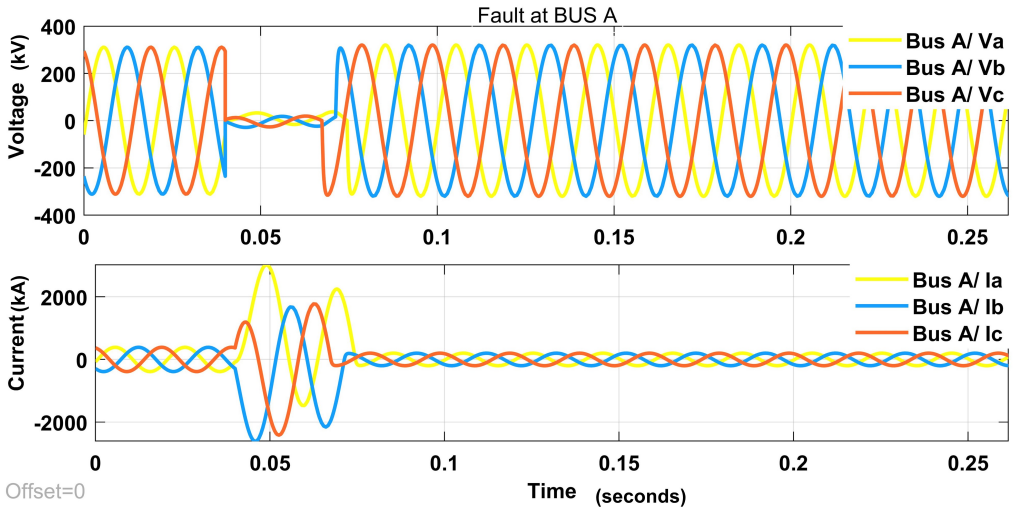

Figure 4. Fault at bus A without the relay.

The application of the instantaneous overcurrent relay has reduced the operating time drastically, thereby protecting the entire system from collapsing.

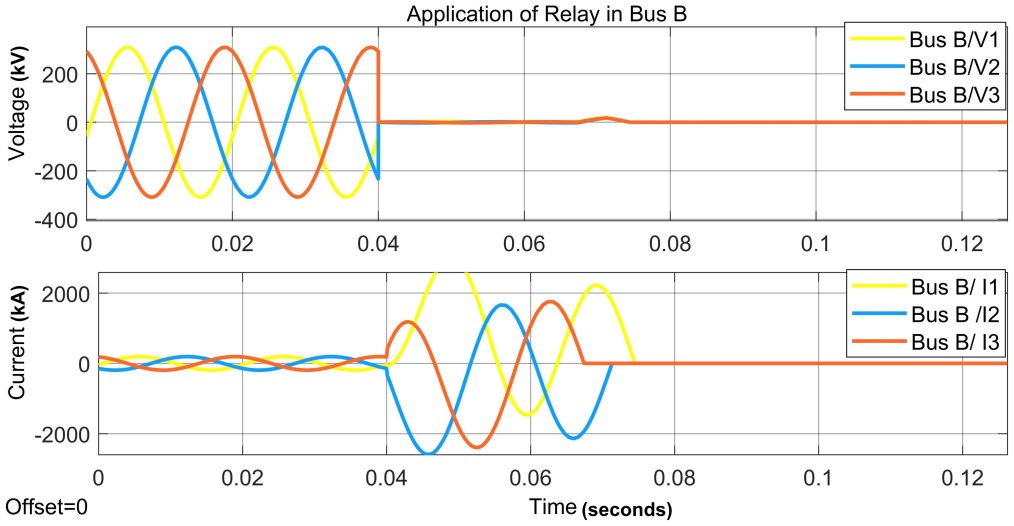

Figure 5. Application of relay at bus B.

The threshold value is an easy way to detect faults and prevent transmission line fault protection tripping delays. The overshoot at Bus B/I_1 in Figure 5 shows that the maximum threshold coefficient was at the highest with 620.4303 kA as seen in Table 2 (AC-G). Additionally, the minimum threshold was at the lowest at the no-fault condition with 10.6870 kA.

The instantaneous overcurrent and voltage relay function model is shown in Figure 6 of relay 1. The trip time for the current is smaller (Figure 6a) compared to the voltage, while the time delay was at zero seconds in each case. This shows a better tripping time than the model without the relay setting, as seen in Figure 4. In addition, the fault current trip time was 0.05 s, while the voltage trip time was 0.35 s, as opposed to 0.04 s in Figures 4 and 5. The reduction of the tripping time was due to the introduction of instantaneous overcurrent and voltage relay settings with the help of the threshold voltage and current of the model.

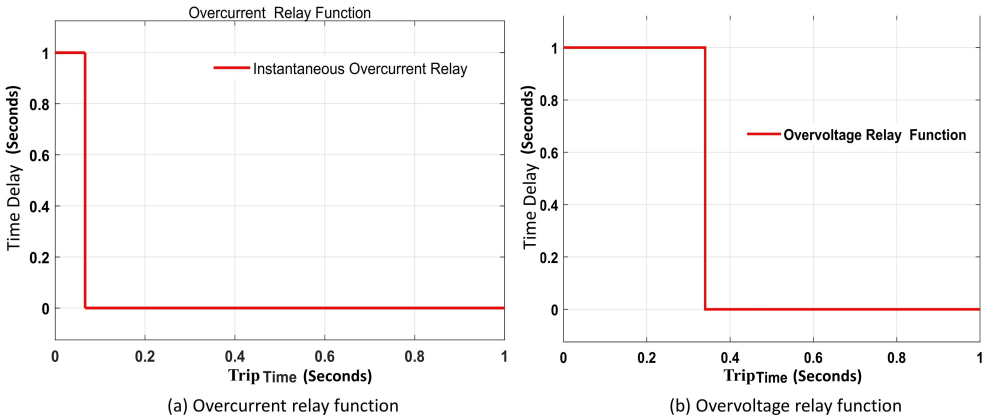

Figure 6. The overcurrent and voltage relay function at relay 1 before setting.

Figure 7 represented the initial condition when the trip time was 0.35 s without setting the instantaneous overvoltage relay at bus B. However, it reduced to 0.05 s when the model was implemented, as shown in Figure 5 above.

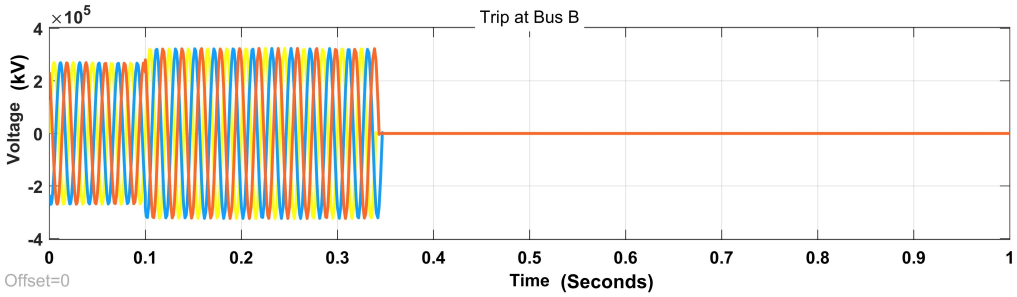

Figure 7. Overvoltage. Trip at Bus B.

In Figure 8, the reference tripping time of the three-phase-to-ground fault at relay 2 shows that the line tripped at 0.2 s without applying the proposed model.

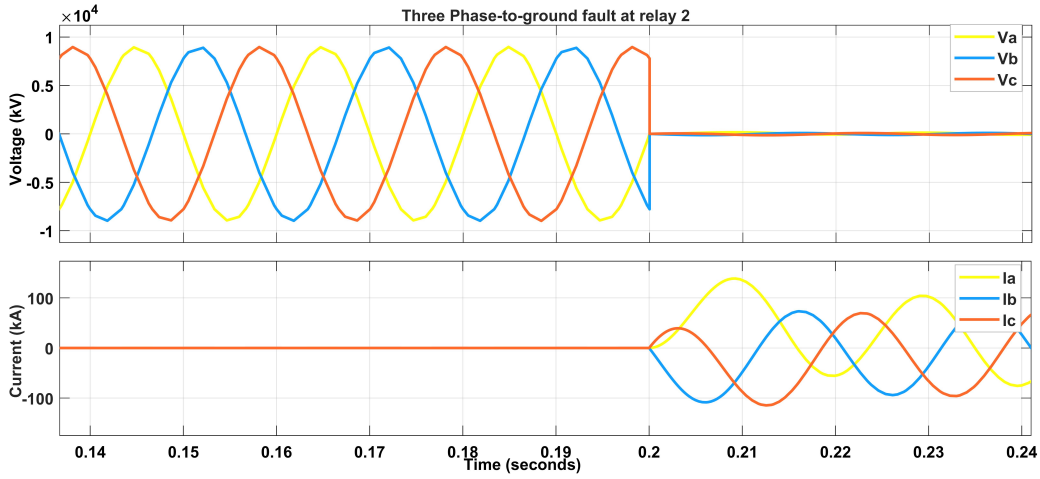

Figure 8. Three phases to ground fault at relay 2.

The performance of the proposed model is shown in Table 7 with a percentage increase in the tripping time without the application of the model compared to the proposed model, and it shows that at bus A, the double line to ground fault shows 99.87% with a difference of 0.33 s. The same also applies to three phase-to-ground faults and to single phase-to-ground faults.

Table 7. Percentage accuracy of the proposed model at bus A.

Fault Types	Trip Time without Proposed Model (Seconds)	Trip Time with Proposed Model (Seconds)	% Increase in Accuracy
L-G	0.25	0.03	85.00
L-L-G	0.38	0.05	99.87
L-L-L-G	0.10	0.04	60.00

The differences in the various fault condition tripping times were computed to find the percentage increment of the tripping time of the normal system without the threshold value. The proposed model is shown in Equation (10) below.

$$P_i = \frac{T_A - T_B}{T_A} \times 100, \tag{10}$$

where P_i is the percentage increment of the tripping time of the relay, T_A is the tripping time without the threshold value, and T_B is the tripping time using the proposed model.

At bus B relay 1, there were significant changes in the tripping time with the double-line-to-ground fault of 84.38% and a difference of 0.27 s, as seen in Table 8. The proposed model improved the tripping time and reduced the time delay of the relay to sense a fault signal and trip, as compared to [16], which focused on the selection and reliance of backup relays to trip in a fault condition.

Table 8. Percentage accuracy of the proposed model at bus B.

Fault Types	Trip Time without Proposed Model (Seconds)	Trip Time with Proposed Model (Seconds)	% Increase in Accuracy
L-G	0.10	0.03	70.00
L-L-G	0.32	0.05	84.38
L-L-L-G	0.20	0.04	80.00

4.2. Comparison of the Proposed Algorithm with the Deep Learning-Based Results

The deep learning-based method was compared with the proposed algorithm for accuracy and tripping time. In [17], an artificial intelligence search algorithm and a genetic algorithm were employed to find the optimal relay setting coordination time. The result shows that the tripping time varied from 0.10 s to 0.69 s at different fault levels. The operating time varied from 0.28 s to 6.3 s at different fault locations. In [18], the Radial Bias Function Neural Network (RBFNN) to learn and detect short-circuit fault current was implemented in the microprocessor of a digital relay on a distribution feeder to detect short-circuit faults using inverter-based distributed energy resources. The offline training time was 0.414 s, the detection time was 0.0136 s, and the trip time was 0.5 s. In [19], a directional overcurrent relay was used at different setting groups to detect faults at various locations. The optimal coordination of directional overcurrent relay in clusters was obtained using a machine learning algorithm and a genetic algorithm, with heuristic adjustment, and the operating time was 497.4069 s. The tripping times were set at 0.282 s and 0.593 s for different clusters. In [20], a dual-path mixed-domain residual threshold network was used for fault diagnosis in bearings, the soft threshold function was employed as the nonlinear transformation layer, and dilated convolution was used to create a dual-path neural network to identify the critical features in the signal without using any signal denoising algorithms. The algorithm's accuracy was about 99.97% on Gaussian noise and 99.98% on real noise. This paper, on the other hand, focused on feature extraction at various

noise levels and thresholds for machine learning training, but the difference lies in the direct application of the proposed model without the combination with other algorithms, as seen in [20], where the channel attention mechanism, spatial attention mechanism, and residual structure were all combined in the dual-path mixed-domain residual threshold network. The soft threshold function was used as the nonlinear transformation layer, and dilated convolution was used to make a dual-path neural network. This was done so that the signal's most important parts could be found without using algorithms to remove noise.

When compared to the literature, the data extraction stage is simpler with the help of the threshold current and voltage and does not require another medium for the extraction of the threshold value; thus, it produces fast and accurate results for the relay setting without needing relay coordination. Additionally, the wavelet transform can de-noise fault signals so that it can be applied to every kind of noise signal.

5. Conclusions

This paper has proposed using the threshold voltage and current value as a standard for coordinating and setting the instantaneous overcurrent relay protection. The simulated result was analysed to confirm the model's viability in calculating the tripping time, delay time and operating time of the high-voltage transmission line relay. It also analyses or detects the maximum and minimum threshold voltage and current suitable for optimising the relay and circuit breaker for optimal performance. This technique helps reduce the time delay and improve the relay's tripping time. One of the constraints of this technique is the inability to optimise the threshold current for different current and voltage types. However, this technique has poor discrimination in distinguishing between fault currents at different points when the fault impedance between two points is small.

Additionally, coordinating is challenging and necessitates changes as the load increases and the optimisation of the model to accommodate different voltage inputs synchronously. This process can be used for all fault types. Therefore, it has a superior and effective tripping time compared to other techniques in the literature.

Author Contributions: Conceptualization, methodology, software, formal analysis, investigation, data curation and writing, V.N.O. Validation, writing—review and editing, visualization, supervision, and project administration, S.H. and K.A.A.G. All authors have read and agreed to the published version of the manuscript.

Funding: This research received no external funding.

Data Availability Statement: Not applicable.

Conflicts of Interest: The authors declare no conflict of interest.

List of Acronyms

TL	Transmission Line
TEC	Thevenin Equivalent Circuit
WT	Wavelet Transform
DWT	Discrete Wavelet Transform
CWT	Continuous Wavelet Transform
SSU	Supply and Switching Unit
IDMT	Inverse Definite Minimum Time
PMU	Phasor Measurement Unit
TMS	Time Multiplier Setting
L-G	Single Phase to Ground Fault
LL-G	Double Phase to Ground Fault
LLL-G	Three Phase to Ground Fault
RBFNN	Radial Bias Function Neural Network

References

1. Matthewman, S.; Byrd, H. Blackouts: A sociology of electrical power failure. *Soc. Space (Przestrz. Społeczna)* **2013**, 31–55.
2. Suliman, M.Y.; Ghazal, M. Design and implementation of overcurrent protection relay. *J. Electr. Eng. Technol.* **2020**, *15*, 1595–1605. [CrossRef]
3. Rojnić, M.; Prenc, R.; Bulat, H.; Franković, D. A Comprehensive Assessment of Fundamental Overcurrent Relay Operation Optimization Function and Its Constraints. *Energies* **2022**, *15*, 1271. [CrossRef]
4. Xu, Z.; Voloh, I.; Khanbeigi, M. Evaluating the impact of increasing system fault currents on protection. In Proceedings of the 2017 70th Annual Conference for Protective Relay Engineers (CPRE), College Station, TX, USA, 3–6 April 2017; pp. 1–20.
5. Ledesma, J.J.G.; de Araujo, L.R.; Penido, D.R.R. A method for evaluation of overcurrent protection in unbalanced distribution systems. *Int. Trans. Electr. Energy Syst.* **2016**, *26*, 412–428. [CrossRef]
6. Draz, A.; Elkholy, M.M.; El-Fergany, A. Over-Current Relays Coordination Including Practical Constraints and DGs: Damage Curves, Inrush, and Starting Currents. *Sustainability* **2022**, *14*, 2761. [CrossRef]
7. Comassetto, L.; Bernardon, D.; Canha, L.; Abaide, A. Software for automatic coordination of protection devices in distribution system. *IEEE Trans. Power Deliv.* **2008**, *23*, 2241–2246. [CrossRef]
8. Chen, C.R.; Lee, C.H.; Chang, C.J. Optimal overcurrent relay coordination in power distribution system using a new approach. *Int. J. Electr. Power Energy Syst.* **2013**, *45*, 217–222. [CrossRef]
9. Andruszkiewicz, J.; Lorenc, J.; Staszak, B.; Weychan, A.; Zięba, B. Overcurrent protection against multi-phase faults in MV networks based on negative and zero sequence criteria. *Int. J. Electr. Power Energy Syst.* **2022**, *134*, 107449. [CrossRef]
10. Jimenez, S.; Vázquez, E.; Gonzalez-Longatt, F. Methodology of Adaptive Instantaneous Overcurrent Protection Setting. *Electronics* **2021**, *10*, 2754. [CrossRef]
11. Esmaili, P.; Zin, A.A.B.M.; Shariati, O. On-line overcurrent relays setting approach in distribution networks by implementing new adaptive protection algorithm. In Proceedings of the 2015 IEEE Tenth International Conference on Intelligent Sensors, Sensor Networks and Information Processing (ISSNIP), Singapore, 7–9 April 2015; pp. 1–6.
12. Guillen, D.; Paternina, M.R.A.; Ortiz-Bejar, J.; Tripathy, R.K.; Zamora-Mendez, A.; Tapia-Olvera, R.; Tellez, E.S. Fault detection and classification in transmission lines based on a PSD index. *IET Gener. Transm. Distrib.* **2018**, *12*, 4070–4078. [CrossRef]
13. Navyasri, G.S.; Deepa, K.; Sailaja, V.; Manitha, P.V. Fault Analysis in Three Phase Transmission Lines using Wavelet Method. In Proceedings of the 2022 6th International Conference on Trends in Electronics and Informatics (ICOEI), Tirunelveli, India, 28–30 April 2022; pp. 248–254.
14. Hemmati, R.; Mehrjerdi, H. Non-standard characteristic of overcurrent relay for minimum operating time and maximum protection level. *Simul. Model. Pract. Theory* **2019**, *97*, 101953. [CrossRef]
15. Erişti, H.; Uçar, A.; Demir, Y. Wavelet-based feature extraction and selection for classification of power system disturbances using support vector machines. *Electr. Power Syst. Res.* **2010**, *80*, 743–752. [CrossRef]
16. Ahmarinejad, A.; Hasanpour, S.M.; Babaei, M.; Tabrizian, M. Optimal overcurrent relays coordination in microgrid using cuckoo algorithm. *Energy Procedia* **2016**, *100*, 280–286. [CrossRef]
17. So, C.; Li, K.; Lai, K.; Fung, K. Application of genetic algorithm to overcurrent relay grading coordination. In Proceedings of the IEE Conference Publication, Edinburgh, UK, 15 May 1998; pp. 283–287.
18. He, L.; Rong, S.; Liu, C. An Intelligent Overcurrent Protection Algorithm of Distribution Systems with Inverter based Distributed Energy Resources. In Proceedings of the 2020 IEEE Energy Conversion Congress and Exposition (ECCE), Virtual, 11–15 October 2020; pp. 2746–2751.
19. Saldarriaga-Zuluaga, S.D.; López-Lezama, J.M.; Muñoz-Galeano, N. Optimal coordination of over-current relays in microgrids using unsupervised learning techniques. *Appl. Sci.* **2021**, *11*, 1241. [CrossRef]
20. Chen, Y.; Zhang, D.; Zhang, H.; Wang, Q.G. Dual-Path Mixed-Domain Residual Threshold Networks for Bearing Fault Diagnosis. *IEEE Trans. Ind. Electron.* **2022**, *69*, 13462–13472. [CrossRef]